Two Improved Color Images Compression Systems

A. A. El-Harby

Department of Mathematics, Faculty of Science, Damietta University
New Damietta, 34517, Egypt
Email: elharby [AT] du.edu.eg

ABSTRACT— ***In this paper, two image compression systems are designed based on quadtree (QT). They can compress the colour images for the three components separately. The proposed systems divides colour images into their three components. Then, the first two components (R and G) are divided into blocks using QT method. While the division of the B component has the same blocks coordinates of the G component. The first system has three minimum values (MVs) and three difference values (DVs) for each block. In the second system for R component, one MV and one DV are identified for every block. While for the other two components, two MVs and one average difference (AD) are determined for any block. As a result, it is found that the division according to the G component is the best giving good compressed images with high compression ratios and visual quality. In addition to, the second system is the best one having the highest performance. This system has the highest accuracy rates in the compression ratios, peak-to-peak signal to noise ratio (PSNR) values, number of blocks and low computational time comparing with the first system.***

Keywords— Quadtree, Color Image Compression, Image Processing

1. INTRODUCTION

Growth of multimedia technology is continuously increased according to the increasing of the demand for image transmission and storage, therefore, efficient image compression is needed to reduce the big amount of required storage and the transmission time [1]. Digital image compression generally divides into two types: lossless and lossy depending on the redundancy type exploited [2-3]. It is employed in many topics such as astronomy [4], remote sensing [5-6], machine vision [7], and real-time system monitoring [8]. The JPEG image compression is widely used based on discrete cosine transform and employs wavelet transform to obtain better compact representations [9-10]. Moreover, many compression systems are designed to be applied on color images. These systems may contain mathematical algorithms or transformations for instance QT [11-12], wavelet [13-14], fractal [15-16] and neural networks [17-18].

QT image compression is an algorithm acting as visual representation for dividing an image into homogenous partitions. These are structured as blocks. Each block must be divided into four equal blocks. The division process ends when all blocks are split according to the division condition and there is no blocks to be split [19-21]. The main advantage of the QT compression technique is the simplicity for indexing and addressing. In addition to it is relatively processed quickly using low specifications of laptop or personal computer [22-23].

Distortion is usually measured by calculating the specified values of PSNR for color images. These values are determined by comparing the original image with the compressed. There are no standard methods for specifying standard definitions of distortion and PSNR for RGB components. The easy method for doing that is applied by averaging the distortions of the three color components [24-25].

In this paper, new two improved compression systems are carried out on color images. The remainder of this paper is organized as follows: in Section 2, the proposed systems are illustrated. Then, section 3 shows experimental results, comparison and discussion. Conclusions are finally made in Section 4

2. PROPOSED SYSTEMS

Two comparison systems are designed according to QT. The systems are applied on the three components of the color image in separated way. In the two systems, the two components R and G are divided based on QT using specified threshold value. If the QT division is verified, the division is continued to specify all blocks. The minimum and maximum values are determined for all blocks. This condition is verified, if the difference value (DV) is greater than the specified threshold value. The DVs are calculated by subtracting the minimum value (MV) from the maximum for each

block as shown in Figure 1. When division process is completed, the top left coordinates (TLC), block sizes and MVs are stored for all blocks. In this case, each block has one MV and one DV. During the division process of the G component, the third component (B) is divided at the same time according to the same coordinates and block size of the second component regardless the QT division condition is verified or not. When division process is completed, two components G & B have the same division of all blocks.

Then, the two systems have two MVs related to the G & B components for each block. Using the first system, the G & B components have two DVs and the other system has only one AD. The values of TLC, block sizes, MVs, DVs and ADVs are stored for divided blocks as specified in Figures 1-2. These two systems are explained in more details in the next sub section.

In order to evaluate the performance of the two proposed systems, the mean squared errors (MSE), the popular PSNR and the compression ratio (CR) are calculated using the same equations in [24].

2.1 Example

This example is introduced to define the two proposed systems clearly. It is carried out on the three components of color image of size 8x8. The two components R and G are divided according to QT. The B component must be divided using the same division structure of G component, even if the division condition is not verified. In the two systems, the R component has one MV and one DV for each block. For instance, the block of coordinates (2, 2) has the MV (45) and the DV (5) as shown in Figures 1-2 and Table 1. In addition to, the two systems have two MVs related to the G & B components for all blocks. While for the first system, the G & B components have two DVs and the other system has only one AD. For instance, the coordinates (4, 2) of the block has the MVs (25, 11), the DVs (5, 1) and one ADV (3) as given in Figures 1-2 and Table 2.

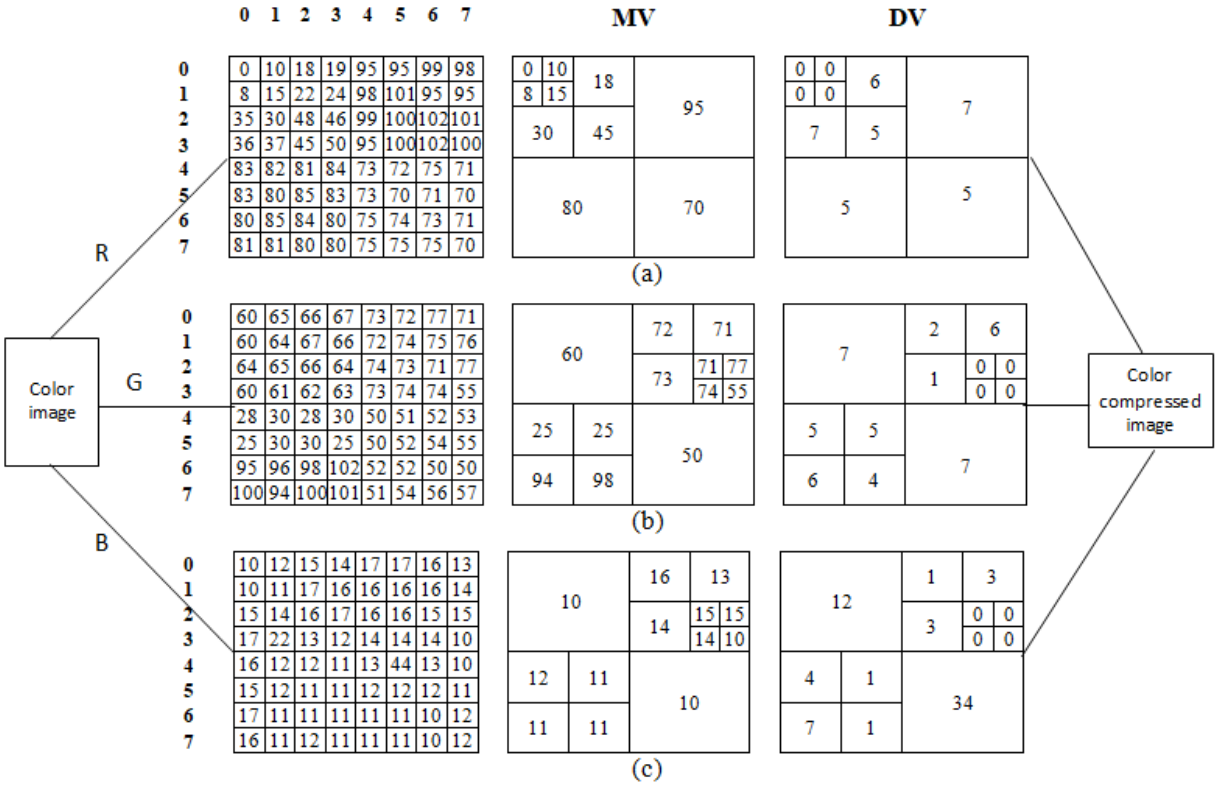

Figure 1: The first System Processing

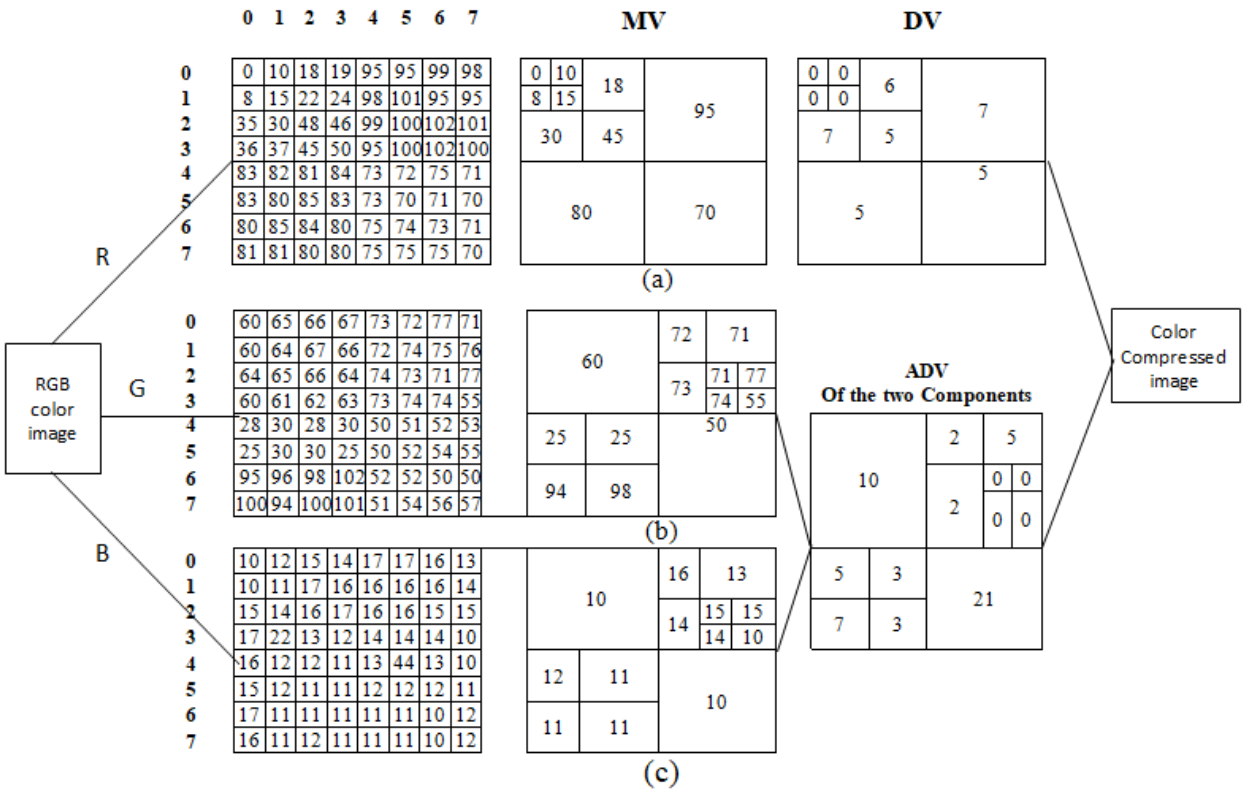

Figure 2: The second System Processing

Table 1: Two systems results of R Component

T L C	Dim	MV of R	DV of R
(0,0)	1	0	0
(0,1)	1	10	0
(1,0)	1	8	0
(1,1)	1	15	0
(0,2)	2	18	6
(2,0)	2	30	7
(2,2)	2	45	5
(0,4)	4	95	7
(4,0)	4	80	5
(4,4)	4	70	5

Table 2: Two systems results of G & B Components

T L C	Dim	MV		DV		ADV
		G	B	$SYS1_G$	$SYS1_B$	$SYS2_G$ and $SYS2_B$
(0,0)	4	60	10	7	12	10
(0,4)	2	72	16	2	1	2
(0,6)	2	71	13	6	3	5
(2,4)	2	73	14	1	3	2
(2,6)	1	71	15	0	0	0
(2,7)	1	77	15	0	0	0
(3,6)	1	74	14	0	0	0
(3,7)	1	55	10	0	0	0
(4,0)	2	25	12	5	4	5
(4,2)	2	25	11	5	1	3
(6,0)	2	94	11	6	7	7
(6,2)	2	98	11	4	1	3
(4,4)	4	50	10	7	34	21

3. RESULTS, COMPARISON AND DISCUSSION

The two systems are carried out on four famous color images (Splash, Lena, Sailboat, and Pepper); see Figure 3. In order to make a real comparison, the same settings are applied of the two system. The dimension of each image is chosen to be 512x512x3 pixels. Forty eight experiments are done with each system using specified threshold values (THV). These values are 0.1, 0.2, 0.3 and 0.5. The obtained results of the two systems are shown in Figures 4-7. Each figure contains four groups. Every one group is specified for one image and has six columns. The first three represents the results of the first system for the three image components. These columns are called $SYS1_R$, $SYS1_G$, and $SYS1_B$. The other three columns represents the results of the second system for the three image components. They are called $SYS2_R$, $SYS2_G$, and $SYS2_B$.

The compression ratio is calculated, getting the size of the original image file divided by the size of the compressed result file. The compression ratios are shown in Table 3. In the first system, they are ranged between 1.1211 and 42.0777, while in the other system, they are ranged between 1.0411 and 40.8765. It is found that the second system has the highest compression ratio. While the obtained values of PSNR are given in the Table 4. In the first system, they are ranged between 44.5564 and 22.6549, while in the second system, the PSNR is between 39.7332 and 16.8528. Finally, the obtained number of blocks values are presented in the Table 5. In the first system, they are ranged between 53820 and 28, while in the second system, the PSNR is between 53820 and 57. The designed programs of the two systems are written using the Matlab software.

In the two systems: it is noticed that the compression ratios decrease when the color images have many details as in the Sailboat image and vice versa; see Table 3 and Figure 8. It is found that the quality of the compressed images and PSNR values are inversely proportional to the compression ratio, as seen in the Figures 4-7. In addition to, the number of blocks decreases if the original image has low details as in the Splash image; see Table 5 and Figure 9. In this respect, the quality of the compressed color images are visually improved when they are divided according to the component G and the CR values are proportional to the THV.

In order to demonstrate comparative results between the two proposed systems and other previous two systems [24]. So, the results of the four systems are compared with respect to the number of blocks at THV=0.5. Figure 10 contains 48 columns, they are organized in 24 pairs. Each pair contains two columns, the first one is specified for the previous work and the next is related to the current work. Every six pairs are specified for one image. The images are Sailboat, Lena, Peppers and Splash respectively. The first three pairs represent the results of the first system in the previous work and current work in that order for the arranged components RGB. The second three pairs represent the results of the second system in the previous work and current work respectively for the arranged components RGB; as shown in the legend. This figure shows that the two proposed systems have lower number of blocks than the two related to previous work. Therefore, the performance of the two proposed system is better than the previous. This means that the design and optimization of the two proposed systems are much better than the other two [24].

Figure 3: Applied Images

Figure 4: Compressed Images using THV=0.1

Figure 5: Compressed Images using THV=0.2

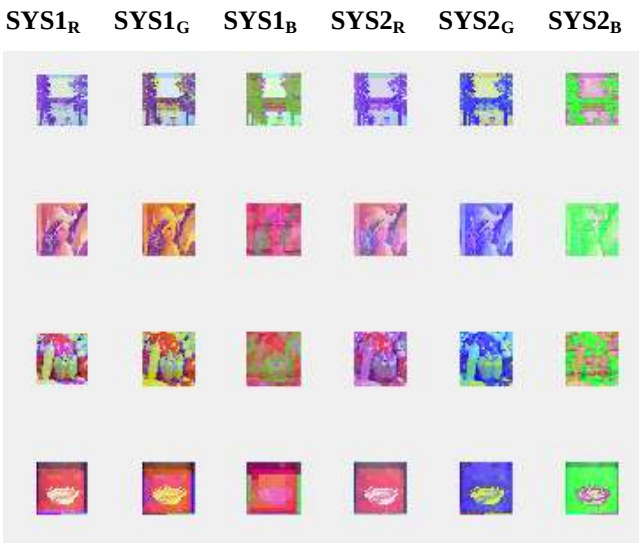

Figure 6: Compressed Images using THV=0.3

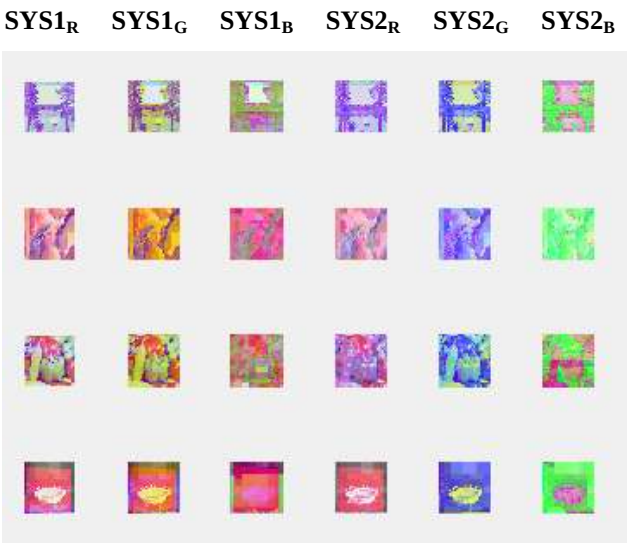

Figure 7: Compressed Images using THV=0.5

Table 3: The obtained compression ratios values

Images Names	**THV (0.1)**						**THV (0.2)**					
	$SYS1_R$	**$SYS1_G$**	**$SYS1_B$**	**$SYS2_R$**	**$SYS2_G$**	**$SYS2_B$**	**$SYS1_R$**	**$SYS1_G$**	**$SYS1_B$**	**$SYS2_R$**	**$SYS2_G$**	**$SYS2_B$**
Sailboat	1.1211	1.1923	1.2916	1.2474	1.0698	1.0411	2.1826	2.4305	2.5566	2.3269	1.8295	1.8028
Lena	2.2161	2.3415	2.4960	2.4141	2.1068	2.0609	4.4997	4.7899	5.3293	5.1907	4.4188	4.2597
Peppers	2.0872	2.1355	2.2518	2.2460	2.1172	2.0747	4.1279	4.3776	4.8846	4.7834	4.1051	3.9513
Splash	4.6611	5.2159	6.0836	5.6734	4.2861	4.0942	8.1108	8.8948	9.4947	8.8224	7.1166	6.9756
Images Names	**THV (0.3)**						**THV (0.5)**					
	$SYS1_R$	**$SYS1_G$**	**$SYS1_B$**	**$SYS2_R$**	**$SYS2_G$**	**$SYS2_B$**	**$SYS1_R$**	**$SYS1_G$**	**$SYS1_B$**	**$SYS2_R$**	**$SYS2_G$**	**$SYS2_B$**
Sailboat	3.3491	3.3756	4.6961	5.4956	5.3243	4.5220	6.9321	7.0174	10.8400	13.5308	12.7727	10.1633
Lena	9.4515	10.0141	12.8317	13.3147	11.1155	10.1281	26.3869	29.9751	42.0777	40.8765	27.9288	25.2248
Peppers	7.1433	7.6626	10.0534	10.3582	8.3155	7.5374	13.7520	15.6504	24.6501	24.9643	16.1007	13.9977
Splash	10.6876	10.8099	14.0680	15.7301	15.1014	13.3710	19.0554	19.9664	32.1710	38.6424	31.3829	25.3392

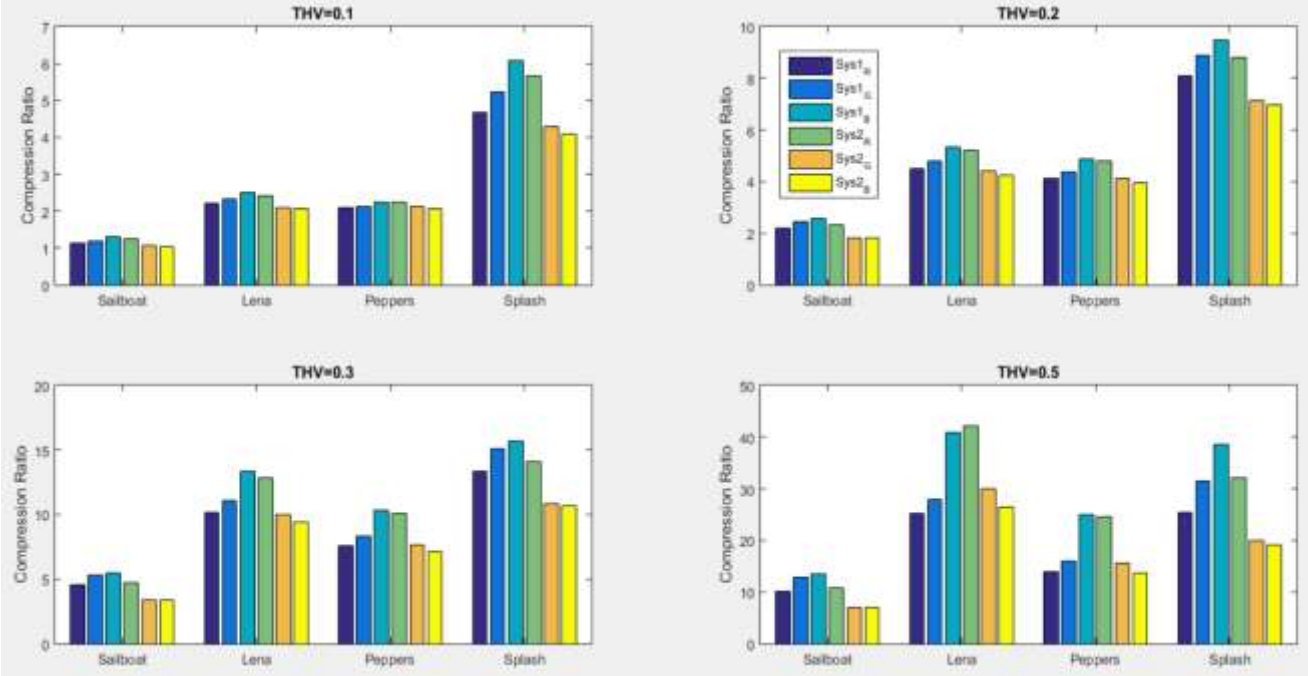

Figure 8: The Obtained Compression Ratios Values

Table 4: The obtained PSNR values

Images Names	THV (0.1)						THV (0.2)					
	$SYS1_R$	$SYS1_G$	$SYS1_B$	$SYS2_R$	$SYS2_G$	$SYS2_B$	$SYS1_R$	$SYS1_G$	$SYS1_B$	$SYS2_R$	$SYS2_G$	$SYS2_B$
Sailboat	37.9080	39.8701	39.8290	33.0613	29.5761	30.4921	32.3360	34.1975	34.3186	30.0984	26.9287	27.8122
Lena	41.7135	43.4086	41.5738	36.4321	26.8637	25.4659	38.2312	36.2503	36.1158	32.6960	24.7260	23.3839
Peppers	40.4202	41.5742	39.3862	29.5019	24.6733	26.0916	34.7582	37.0066	34.5127	27.1942	22.7794	23.4725
Splash	44.5564	42.0062	40.4955	39.7332	24.0579	22.5220	37.6665	36.3442	35.2249	35.2946	21.3511	20.0523
Images Names	**THV (0.3)**						**THV (0.5)**					
	$SYS1_R$	$SYS1_G$	$SYS1_B$	$SYS2_R$	$SYS2_G$	$SYS2_B$	$SYS1_R$	$SYS1_G$	$SYS1_B$	$SYS2_R$	$SYS2_G$	$SYS2_B$
Sailboat	27.3193	28.9501	28.6541	26.3825	24.9360	25.2133	22.6549	24.0312	23.6926	22.1352	22.5435	22.2914
Lena	31.9621	32.0483	30.3525	27.5573	22.5763	21.4120	26.6808	25.8129	25.1905	23.0978	20.4710	19.6196
Peppers	30.0310	31.3521	29.4387	24.9573	21.5083	21.0628	25.4803	27.2285	24.7669	22.1887	19.8862	18.6204
Splash	31.9337	30.3640	30.4221	29.1847	19.2357	18.6990	26.2865	25.9466	27.1998	27.2550	16.8528	17.5116

Table 5: The obtained number of blocks values

Images Names	THV (0.1)						THV (0.2)					
	$SYS1_R$	$SYS1_G$	$SYS1_B$	$SYS2_R$	$SYS2_G$	$SYS2_B$	$SYS1_R$	$SYS1_G$	$SYS1_B$	$SYS2_R$	$SYS2_G$	$SYS2_B$
Sailboat	53820	27475	27475	45716	45716	53820	24516	6793	6793	24674	24674	24516
Lena	20631	12574	12574	17110	17110	20631	7531	3520	3520	5882	5882	7531
Peppers	20408	14000	14000	15793	15793	20408	9403	5050	5050	6199	6199	9403
Splash	8323	3661	3661	7574	7574	8323	5346	2332	2332	5148	5148	5346
Images Names	**THV (0.3)**						**THV (0.5)**					
	$SYS1_R$	$SYS1_G$	$SYS1_B$	$SYS2_R$	$SYS2_G$	$SYS2_B$	$SYS1_R$	$SYS1_G$	$SYS1_B$	$SYS2_R$	$SYS2_G$	$SYS2_B$
Sailboat	8290	975	975	10036	10036	8290	1580	133	133	1605	1605	1580
Lena	2091	558	558	1382	1382	2091	388	28	28	57	57	388
Peppers	4467	1828	1828	2113	2113	4467	1994	658	658	529	529	1994
Splash	3481	1126	1126	3146	3146	3481	1638	342	342	1022	1022	1638

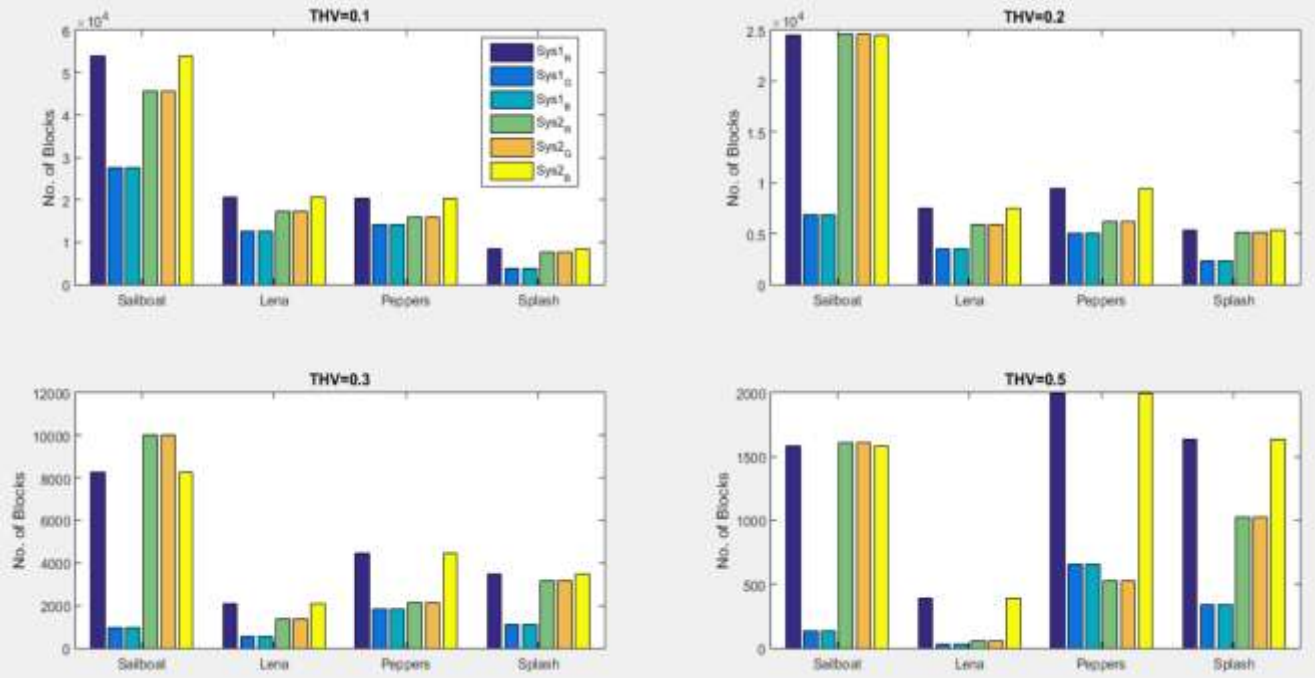

Figure 9: The Obtained Number of Blocks Values

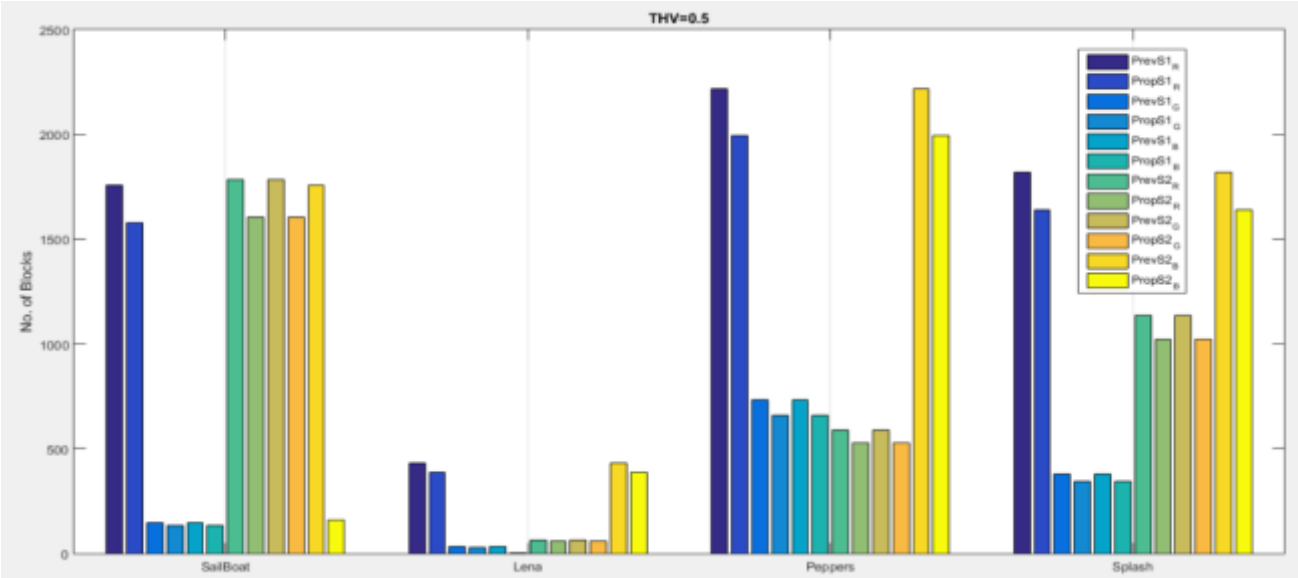

Figure 10: Comparison of Number of Blocks among the two Proposed Systems and the Previous two [24]

4. CONCLUSIONS

This paper presents a new two improved compression systems for color images. They have the ability to separate the colour images components and compress them in systematic way. Where, the R and G components are divided based on QT, the other component is divided using the same division of the G component even if the condition of QT division is not verified. In all experiments, the two proposed systems are carried out on four famous images used in many compression works. After analyzing all the results obtained by calculating the compression ratios, PSNR and number of blocks. It is obvious that the compression ratios of color images are extremely increased by increasing the THVs while the visual and quality of the compressed color images may be affected. It is also found, the division of blocks according to the G component is the best one with good vision and quality of the compressed images having high compression ratios. In addition to, the performance of the second system is the best by reaching the highest accuracy rates in the compression ratios, PSNR values, number of blocks and least computational time comparing with the first proposed system; see the analyzed results in Figures 4-9 and Tables 3-5. It is found that the proposed two systems have high compression ratios, low number of blocks and low processing time comparing with the previous two systems [24].

5. REFERENCES

[1] Shikang Kong, Lijuan Sun, Chong Han, Jian Guo, "An Image Compression Scheme in Wireless Multimedia Sensor Networks Based on NMF", Information, vol. 8, no. 26, pp.1-14, 2017.
[2] Mansour Nejati, Shadrokh Samavi, Nader Karimi, Sayed Mohammad Reza Soroushmehr, Kayvan Najarian, "Boosted Dictionary Learning for Image Compression", IEEE TRANSACTIONS ON IMAGE PROCESSING, vol. 25, no. 10, pp. 4900-4915, 2016.
[3] Miguel Hernández-Cabronero, Ian Blanes, Armando J. Pinho, Michael W. Marcellin, Joan Serra-Sagristà, "Progressive Lossy-to-Lossless Compression of DNA Microarray Images", IEEE SIGNAL PROCESSING LETTERS, vol. 23, no. 5, pp. 698-702, 2016.
[4] Petr Pata, Jaromir Schindler, "Astronomical context coder for image compression", Experimental Astronomy, vol. 39, no. 3, pp 495-512, 2015.
[5] CuipingShi, JunpingZhang, Ye Zhang, "Content-based onboard compression for remote sensing images", Neurocomputing, vol. 191, pp. 330-340, 2016.
[6] Ke-KunHuang, HuiLiu, Chuan-XianRen, Yu-FengYu, Zhao-RongLai, "Remote sensing image compression based on binary tree andoptimized truncation", Digital Signal Processing, vol. 64, pp. 96-106, 2017.
[7] Charles Z. Liu, Manolya Kavakli, "Extensions of principle component analysis with applications on vision based computing", Multimedia Tools and Applications, vol. 75, no. 17, pp 10113-10151, 2014.
[8] Jing Tang, Yun'an Hu, Tao Lin, Yongxing Xie, "Electronic Equipment Real-time Monitoring System Design based on Huffman compression principle", 2nd International Conference on Signal Processing Systems (ICSPS), pp. 763-765, 2010.
[9] Mohammad-Shahram Moin, "Face recognition in JPEG compressed domain: a novel coefficient selection approach", Signal, Image and Video Processing, vol. 9 , no. 3, pp 651-663, 2015.
[10] Rong Zhang, Rang-Ding Wang, "In-camera JPEG compression detection for doubly compressed images", Multimedia Tools and Applications, vol. 74, no. 15, pp 5557-5575, 2015.
[11] SanuThomas, ThomaskuttyMathew, "Lossless address data compression using quadtree clustering of the sensors in a grid based WSN", Ad Hoc Networks, vol. 56, pp. 84-95, 2017.
[12] Xingsong Hou a,n, MinHan a, ChenGong b, XuemingQian, "SAR complex image data compression based on quadtree and zerotree Coding in Discrete Wavelet Transform Domain: A Comparative Study", Neurocomputing, vol. 148, pp. 561-568, 2015.
[13] WeiMA, XunLIU, "Improving the efficiency of DAMAS for sound source localization via wavelet compression computational grid", Journal of Sound and Vibration, vol. 395, pp. 341-353, 2017.
[14] K. Srinivasan, Justin Dauwels, M. Ramasubba Reddy, "Multichannel EEG Compression: Wavelet-Based Image and Volumetric Coding Approach", IEEE JOURNAL OF BIOMEDICAL AND HEALTH INFORMATICS, vol. 17, no. 1, pp. 113-120, 2013.
[15] Mamata Panigrahy, Indrajit Chakrabarti, A. S. Dhar, "Low-Delay Parallel Architecture for Fractal Image Compression", Circuits, Systems, and Signal Processing, vol. 35, no. 3, pp 897-917, 2016.
[16] VijayshriChaurasia, VaishaliChaurasia, "Statistical feature extraction based technique for fast fractal image compression", Journal of Visual Communication and Image Representation, vol. 41, pp. 87-95, 2016.
[17] Mayur Prakash, Deepak Arora, "An Approach Towards Lossless Compression Through Artificial Neural Network Techinique", Int. Journal of Engineering Research and Applications, vol. 5, no. 7 (Part-1), pp.93-99, 2015.
[18] Abir JaafarHussain, DhiyaAl-Jumeily, NaeemRadi, PauloLisboa, "Hybrid Neural Network Predictive-Wavelet Image Compression System", Neurocomputing, vol. 151, pp.975-984, 2015.
[19] Hui Li Tan, Chi Chung Ko, Susanto Rahardja, "Fast Coding Quad-Tree Decisions Using Prediction Residuals Statistics for High Efficiency Video Coding (HEVC)", IEEE TRANSACTIONS ON BROADCASTING, vol. 62, no. 1, pp. 128-133, 2016.
[20] Hamid Reza Tohidypour, Mahsa T. Pourazad, Panos Nasiopoulos, "Probabilistic Approach for Predicting the Size of Coding Units in the Quad-Tree Structure of the Quality and Spatial Scalable HEVC", IEEE TRANSACTIONS ON MULTIMEDIA, vol. 18, no. 2, pp. 182-195, 2016.
[21] El-Harby A.A., Behery G.M., "Qualitative Image Compression Algorithm Relying on Quadtree", International Journal on Graphics, Vision and Image processing (GVIP), vol. 8, no. 3, pp. 41-50, 2008.
[22] Tamer Rabie, Ibrahim Kamel, "Toward optimal embedding capacity for transform domain steganography: a quad-tree adaptive-region approach", Multimedia Tools and Applications, vol. 76, no. 6, pp 8627-8650, 2017.
[23] Yu-Chen Hu, Ji-Han Jiang, "Low-complexity progressive image transmission scheme based on quadtree segmentation", Real-Time Imaging, vol. 11, no. 1, pp.59-70, 2005.
[24] El-Harby A. A., Behery G. M., "Novel Color Image Compression Algorithm Based on Quad tree", Global Journal of Computer Science and Technology (F), Volume 12, no. 13, Version 1.0, PP. 13-22, 2012.
[25] Hui Liu, Ke-Kun Huang, Chuan-Xian Ren, Yu-Feng Yu, Zhao-Rong Lai, "Quadtree coding with adaptive scanning order for space-borne image compression", Signal Processing: Image Communication, vol. 55, pp. 1-9, 2017.